Quaternary Science Reviews 124 (2015) 68–83

Contents lists available at ScienceDirect

Quaternary Science Reviews

journal homepage: www.elsevier.com/locate/quascirev

Reconstructing water level in Hoyo Negro, Quintana Roo, Mexico, implications for early Paleoamerican and faunal access

S.V. Collins [a, *], E.G. Reinhardt [a], D. Rissolo [b], J.C. Chatters [c], A. Nava Blank [d], P. Luna Erreguerena [e]

[a] School of Geography and Earth Sciences, McMaster University, Hamilton, Ontario, Canada
[b] Center of Interdisciplinary Science for Art, Architecture, and Archaeology (CISA3), Qualcomm Institute, UCSD Division of Calit2, University of California, San Diego, USA
[c] Applied Paleoscience and DirectAMS, 10322 NE 190th Street, Bothell, WA 98011, USA
[d] Bay Area Underwater Explorers, CISA3/UCSD, Berkeley, CA, USA
[e] Subdirección de Arqueología Subacuática, Instituto Nacional de Antropología e Historia, 06070 Mexico City, Mexico

ARTICLE INFO

Article history:
Received 11 February 2015
Received in revised form
19 June 2015
Accepted 20 June 2015
Available online xxx

Keywords:
Cave sediments
Paleoamericans
Anchialine
Hoyo Negro
Paleoenvironmental reconstruction
Yucatan
Glacioeustasy
Holocene sea-level

ABSTRACT

The skeletal remains of a Paleoamerican (Naia; HN5/48) and extinct megafauna were found at −40 to −43 mbsl in a submerged dissolution chamber named Hoyo Negro (HN) in the Sac Actun Cave System, Yucatan Peninsula, Mexico. The human remains were dated to between 12 and 13 Ka, making these remains the oldest securely dated in the Yucatan. Twelve sediment cores were used to reconstruct the Holocene flooding history of the now phreatic cave passages and cenotes (Ich Balam, Oasis) that connect to HN. Four facies were found: 1. bat guano and Seed (SF), 2. lime Mud (MF), 3. Calcite Rafts (CRF) and 4. Organic Matter/Calcite Rafts (OM/CRF) which were defined by their lithologic characteristics and ostracod, foraminifera and testate amoebae content. Basal radiocarbon ages (AMS) of aquatic sediments (SF) combined with cave bottom and ceiling height profiles determined the history of flooding in HN and when access was restricted for human and animal entry. Our results show that the bottom of HN was flooded at least by 9850 cal yr BP but likely earlier. We also found, that the pit became inaccessible for human and animal entry at ≈8100 cal yr BP, when water reaching the cave ceiling effectively prevented entry. Water level continued to rise between ≈6000 and 8100 cal yr BP, filling the cave passages and entry points to HN (Cenotes Ich Balam and Oasis). Analysis of cave facies revealed that both Holocene sea-level rise and cave ceiling height determined the configuration of airways and the deposition of floating and bat derived OM (guano and seeds). Calcite rafts, which form on the water surface, are also dependent on the presence of airways but can also form in isolated air domes in the cave ceiling that affect their loci of deposition on the cave bottom. These results indicated that aquatic cave sedimentation is transient in time and space, necessitating extraction of multiple cores to determine a limit after which flooding occurred.

1. Introduction

In 2007, cave divers Alberto NavaBlank, Alex Alvarez and Franco Attolini were exploring a previously unmapped section of the Sac Actun Cave System in Quintana Roo, Mexico (Fig. 1). During exploration, they discovered a 55 m (maximum) deep underwater pit they named Hoyo Negro (HN; Chatters et al., 2014). At the bottom of the pit were the remains of at least 26 large mammals including extinct Pleistocene megafauna (e.g. extinct: sabertooth [Smilodon fatalis], gomphothere [Cuvieronius cf. tropicus, a proboscidean], Shasta ground sloth [Nothrotheriops shastensis]; a bear of the genus Tremarctos and sloth of the family Megalonychidae; extant: puma, bobcat, coyote, Baird's tapir, collared peccary and white-nosed coati, (Chatters et al., 2014). Amongst this Lagerstätten of terrestrial animals, were the remains of a 15–16 year old woman whom the dive team named Naia (HN5/48; Chatters et al., 2014). U/Th dating of calcite florets that had precipitated on the bones post-mortem provided a minimum age of 12 ± 0.2 Ka, while AMS

* Corresponding author. Present address: University of Toronto Mississauga, Department of Chemical & Physical Sciences, Mississauga, Ontario, L5L 1C6, Canada.
E-mail address: shawnvcollins@icloud.com (S.V. Collins).

http://dx.doi.org/10.1016/j.quascirev.2015.06.024
0277-3791/

Fig. 1. The location of Cenote Ich Balam, which was used to access Hoyo Negro, on the Yucatan Peninsula, Mexico.

radiocarbon ages of tooth enamel bioapatite provided a maximum age of 13 Ka. Naia's craniofacial similarity with other Paleoamericans and her Beringian-derived mtDNA contribute to the debate on the arrival and dispersal of early humans in North and South America (see Chatters et al., 2014) for a full discussion; Anderson and Gillam, 2000; Chatters, 2000; Dixon, 1999; González et al., 2008). As summarized in Chatters et al. (2014), the Yucatan caves provide a unique environment for preservation that is unparalleled. Few early Paleoamerican remains have been found in terrestrial sites and none have been associated with extinct megafauna (Chatters et al., 2014; González et al., 2013; Chatters, 2000). However, radiocarbon dating bone material found in the flooded Yucatan caves is not without complications (see Chatter et al., 2014). Hard-water effects and collagen leaching result in contamination which can make dating difficult (e.g. Dixon, 1999; González et al., 2008; Taylor, 2009). Dating of associated artifacts can be used, but is problematic, particularly in HN, were there is little sediment coverage to provide any stratigraphic association or context (Chatters, 2000; Chatters et al., 2014). In Naia's case, there was insufficient bone collagen for radiocarbon dating necessitating the use of small quantities of tooth enamel. Her age was constrained using U-Th dating of calcite florets that formed on the bones postmortem and with water level reconstructions from cave deposits (as presented in Chatters et al., 2014).

The goal of this study was to provide constraining data on Naia's age through reconstructing water levels in the cave as her taphonomic condition indicated she fell and died in water at the bottom of HN (Chatters et al., 2014). We also contribute to understanding site formation history for further studies on the HN Lagerstätten.

1.1. Geologic setting

The Yucatan Peninsula, Mexico is a large Paleogene to Quaternary limestone platform with an area of over 350,000 Km^2, of which half is submerged under the Gulf of Mexico (Weidie, 1985). Metamorphic basement rocks underlie the Cenozoic units (Ward et al., 1995). The limestone platform has been largely unaffected by tectonic uplift or orogenic events as bedding is largely subhorizontal with minimal differential tilting (Beddows, 2004; Coke et al., 1991).

In the Yucatan, as with other anchialine settings, the aquifer is density stratified and composed of a freshwater meteoric lens sitting on top of saline water. Marine water intrudes from the coast via the permeable limestone with the fresh (or slightly brackish) meteoric water mass thickening landward and separated by a halocline (underground estuary; Moore, 1999). Density contrasts between the warmer, denser saline water (PSU 35) and the cooler freshwater (PSU <1) lens are responsible for the stratification (Esterson, 2003; Collins et al., 2015a). The main interface (halocline) between the two water bodies is termed the mixing zone and has PSU values ranging from 1 to 35 (Collins et al., 2015a; Werner, 2007). The mixing zone can have changes in temperature, pH, dissolved oxygen and salinity depending on the location in the cave and the time of year (Esterson, 2003). The meteoric and marine water masses have uniform characteristics. Mixing occurs at the halocline through a variety of mechanisms including tidal pumping, precipitation patterns, cave conduit roughness etc., which produces spatial variation in meteoric salinity but with a gradient inland (e.g. Yax Chen @ 6 PSU vs Hoyo Negro @ 1 PSU; Collins et al.,

2015a, b; Chatters et al., 2014). Hoyo Negro is ≈ 7 km from the coast and has a halocline at 15–22 m depth while Yax Chen is ≈1.5 km inland and its halocline is at 10 m (Collins et al., 2015a, b). Groundwater level rises gradually away from the coast (10–15 cm/km; ≈1–2 m above msl at HN). Due to the high hydraulic conductivity of the limestone the flow velocities in the meteoric lens are typically low (generally <6 cm/s; Beddows, 2004; Moore, 1999). No rivers drain the Yucatan because rainfall quickly penetrates through the permeable vadose zone to the water table (Bauer-Gottwein et al., 2011). Studies of the water table response to external forcing mechanisms in the Northwestern Yucatan have shown that sea-level is a controlling factor on water table fluctuations (Perry et al., 1989, 1995, 2003). However, fault and fracture zones (Rio Hondo, Holbox) are thought to influence water flow (Kambesis and Coke, 2013).

Cave and cenote formation has been attributed to processes driven by glacio-eustatic sea-level cycles (Beddows, 2004; Smart et al., 2006). Meteoric water was found to be saturated with respect to calcite ($CaCO_3$) until mixed with saline groundwater. In the mixing zone, the water was undersaturated with respect to $CaCO_3$ resulting in dissolution of limestone and cave passage enlargement (Beddows, 2004; Smart et al., 2006; Back et al., 1986; Hanshaw and Back, 1980; Back et al., 1979). Smart et al. (2006) studied cave speleothems and determined that numerous cycles of subaqueous/subaerial conditions had occurred over the life of the cave passages, as evidenced by repeated sequences of dissolution and recrystallization.

1.2. Hoyo Negro - Sac Actun Cave system

Hoyo Negro (HN) is a dissolution feature found in the Outland Cave, which is part of Sac Actun, the world's second longest subaqueous cave system (220 km), (Quintana Roo Speleological Survey, 2013) located in the Mexican state of Quintana Roo, near the town of Tulum (Fig. 1). The Outland Cave is part of a network of over 1000 km of anastomosing phreatic caves that trend sub-perpendicular to the Caribbean Coast from Puerto Morelos to Miyul (Kambesis and Coke, 2013). As the anastomosing conduits drain the upland areas, flow is generally to the east towards the coast (Neuman and Rahbek, 2007). HN is a bell shaped dissolution chamber with a diameter of 32 m at the top and 62 m near the bottom. The rim of the pit is located at a water depth of approximately −12 m while the bottom ranges from −33 m on the north wall to -48 m on the south wall but has crevices that extend to −55 m (Chatters et al., 2014). Three phreatic cave passages merge into HN. Such cross-linked passages are common in the anastomosing network of the Yucatan (Fig. 2a). The passages have an approximate mean depth of −12 m, with sidewall widths that are >10 m in some instances. This elliptical tabular morphology is a common passage type in the Yucatan (Smart et al., 2006) and generally does not follow bedding planes. The wide horizontal shape is a result of dissolution in the mixing zone and shows little evidence of past flow direction or velocities (Smart et al., 2006). However, the northeast-southwest Rio Hondo Fault Zone may have also influenced cave passage development in Sac Actun, but there is no definitive study of this feature (Kambesis and Coke, 2013; Weidie, 1985). From the pit the northeast passage leads to Cenote La Concha which is over ≈600 m upstream from HN but has a very narrow passage (Fig. 2a). The downstream southeast passage, which is wider than La Concha, leads to Cenotes Ich Balam (60 m) and Oasis (≈600 m; Chatters et al., 2014).

1.3. Paleoamerican remains in Hoyo Negro

HN was not the first significant Paleoamerican site found in the submerged caves of the Yucatan Peninsula. González et al. (2013) reports that, to-date, eight prehistoric sites with human remains have been discovered in the caves in the Tulum region, Mexico. Currently, (with the exception of HN) none of these human remains have been reported to be associated with any fauna of Pleistocene age. Indirect evidence of Paleoamerican occupation, such as charcoal, fossil animal bones and lithic tools, is reported but not in association with the skeletons (González et al., 2008). HN is the first prehistoric site where both human and extinct Pleistocene megafauna skeletal material have been found co-mingled (Chatters et al., 2014).

Previous to the discovery of Naia, the most significant find in the Yucatan was the human remains of a female found in Naharon Cave by Jim Coke and Tom Young. She was 80% intact and was considered to be in fair taphonomic condition (González et al., 2008). Radiocarbon dating of amino acids indicated that the remains were from 13.4 to 13.8 Ka (González et al., 2013) although the age has been questioned due to the leaching and degradation of amino acids necessary to calculate an accurate date (Chatters et al., 2014; Taylor, 2009). No primary environmental data were collected to assess its taphonomic history or the skeletal age.

In the case of HN, there were questions on how Naia and the animals entered the cave system and ultimately fell into the pit, with the possibilities including accidental (trap; cenote Ich Balam) and/or a “willing” entry scenarios (Cenotes Oasis and La Concha). The three cave passages leading to Hoyo Negro are relatively shallow at ≈ −12 mbsl. The bottom has irregular topography due to the ceiling breakdown, with the scattered but intact skeletal material lying on and in crevices between the limestone blocks. The closest entry point was Ich Balam located 60 m downstream of the pit, followed by Cenotes Oasis (≈600 m) and La Concha (≈600 m; Fig. 2a). Both La Concha and Oasis have enlarged central pits that are open to the surface due to the collapse of the cavern ceiling. They have low, sloping walls and cave passages that are open at ground level, providing easy access for animals or humans (Chatters et al., 2014; Finch, 1965). The entrance of Ich Balam measures only 1.2 × 5 m and is located at the apex of the ceiling in an otherwise roofed cavern. Branches and leaves could have concealed the opening, allowing unsuspecting animals to fall 8 m to the cavern floor. The domed shape of the cavern roof, with its speleothem coated walls, would have prevented escape for any animals that survived the fall, forcing movement through either of the two existing cave passages present in Ich Balam. If they chose poorly, unsuspecting animals would fall into HN. This would be applicable for smaller fauna such as cats but not for the larger gomphotheres or sloths. Animals may have “willingly” entered the dark cave passage, attracted by the smell of groundwater, or in the case of the carnivores, the cries of animals in distress or the smell of carrion, and may have inadvertently fallen into the pit. Oasis and La Concha entry points are the farthest away (i.e. ≈ 600 m) necessitating navigating long and sometimes restricted passages in the dark.

The skeletons found at HN are well-preserved, but most are not articulated. Many disarticulated skeletons display evidence of impact trauma, suggesting they fell into water and progressively decayed, with body parts falling in different parts of the pit as the corpses floated on the surface. The lower half of Naia showed greater articulation, suggesting that this portion of the skeleton settled intact and decomposed in situ. There is no significant speleothem other than calcite florets covering most of the skeletons, suggesting the skeletons were deposited in water or quickly became covered by rising water levels. However, during our investigations there were many questions about when the pit flooded, and how water levels may have fluctuated or whether they reflected Holocene sea-level changes.

Our research throughout the investigation of HN was to provide the environmental context of site evolution while assessing

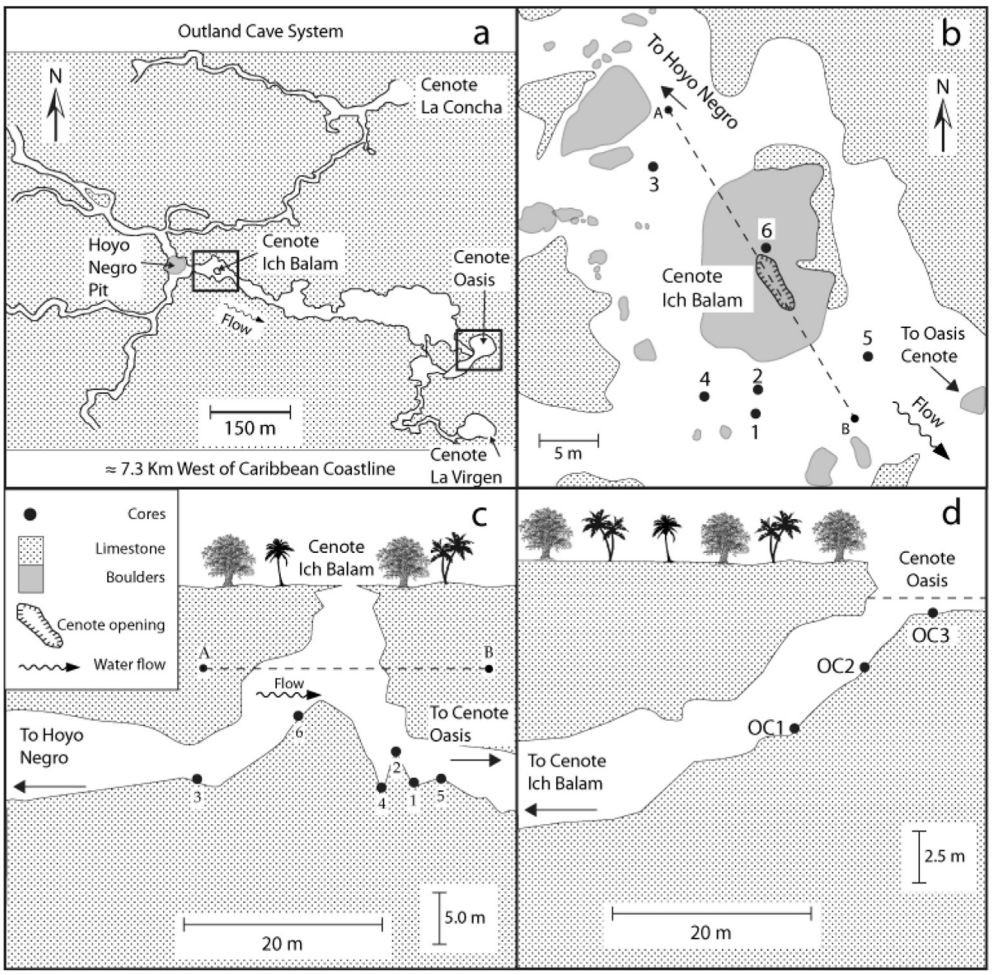

Fig. 2. a) The Outland Cave in the Sac Actun Cave System showing the cave passage geometry and proximity of Cenotes Ich Balam, Oasis, La Concha and La Virgen to Hoyo Negro (HN). b) Plan view of Ich Balam showing core locations and cave features. Sediment coverage is predominantly on the breakdown pile in the central area of the cenote. c, d) Cross-section of core locations in Cenote Oasis and Ich Balam (vertical exaggeration = 4 and 8, respectively).

entry points and determining when HN was ultimately inaccessible as a result of rising water levels. We accomplished this through dating aquatic sediments in HN, cave passages and the cenotes Ich Balam and Oasis, and by reconstructing water levels and sedimentation patterns in the context of the cave configuration. This provided important water level information for assessing the age of Naia, but also provides a minimum age for the faunal accumulation in HN. This research will be important for future studies addressing site formation and taphonomy of the skeletal material in similar sites, not only in the Yucatan but also worldwide (e.g. Gabriel et al., 2009; Gregory et al., 2015; Hodell et al., 2005; Peros et al., 2007).

1.4. Cave sedimentation and microfossil proxies

Aqueous cave sedimentation is an area of research that is underdeveloped in terms of the process and contributing factors. Yucatan cave sediment contains minimal amounts of siliciclastics, being composed largely of either organic matter (OM) or secondarily precipitated calcite rafts. OM enters the cave via transport from terrestrial sources or through primary productivity in sunlit cenote water bodies while calcite rafts form on surface waters in cenotes or in air domes in the cave (Collins et al., a, b; van Hengstum et al., 2010; Taylor and Chafetz, 2004; van Hengstum et al., 2015). Gabriel et al. (2009) was the first to examine how water level affected cenote development in the Yucatan while van Hengstum used microfossils (foraminifera and testate amoebae) and cave sediment records to reconstruct groundwater salinity over the past 4.5 Ka (van Hengstum et al., 2009b; van Hengstum et al., 2008; van Hengstum et al., 2010). Subsequent work in Bermuda and Bahamas used similar techniques (van Hengstum et al., 2011; van Hengstum et al., 2009a; van Hengstum et al., 2013). However, many of the previous ideas relating cave sedimentation to sea-level were inferred from limited background data (e.g. Bermuda; van Hengstum et al., 2011; also van Hengstum et al., 2009a; Bahamas; van Hengstum et al., 2013). Subsequent research by Collins et al. (2015a,b) was conducted to enhance this body of research documenting sources and controls of sedimentation in Yax Chen (part of the nearby Ox Bel Ha Cave System) and its relationship with an extensive mangrove system and with a recent hurricane (Ingrid Sept 2013; Collins et al., 2015a,b). The results from HN provide an extension of that research, but in a cave system where terrestrial vegetation dominates (forest vs mangrove) and where sedimentation is more focused and less extensive. The HN results are unique; as they take into account both the bottom and ceiling heights of the cave showing its role in focusing OM and calcite raft deposition, a factor that has not been considered previously.

2. Methods

2.1. Field

Twelve push cores (5 cm diam, 11–136 cm long) were obtained from Ich Balam, Oasis, HN and the passage leading from Ich Balam to HN using SCUBA (Self-Contained Underwater Breathing Apparatus). All cores reached refusal on the underlying cave subsurface (Fig. 2b–d). In order to develop a flooding history of the cave, core locations were selected according to three criteria: spatial coverage, the availability of sediment, and depth. Core sites tended to be focused close to the cenotes where accumulations are thicker, as opposed to the cave passages that contained no or very thin (<1 cm) sediment coverage. Sediment coverage in HN consisted of isolated calcite raft piles and concentrations of OM including seeds, branches and charcoal, which were concentrated in small piles and scattered on the cavern floor as well as on limestone and speleothem ledges along the sides of the cavern. The HN core (C9) was taken through one of the calcite raft piles on the roof breakdown. Core compaction was measured before removal and averaged ≈50% which is typical of cave sediments in the Yucatan (Gabriel et al., 2009; van Hengstum et al., 2010). Core sites were positioned using previously collected cave maps of the sites with depths measured using a digital depth gauge (±10 cm precision).

Cave passage profiles were measured at tie-off points along the cave line which were installed during initial exploration of the cave. At each tie-off, ceiling and bottom elevation were measured with a digital depth gauge. Sidewall dimensions were also measured with a tape measure from tie-off points. Line azimuth (compass) and also distance between tie-off points were measured providing an overall orientation and distance of the cave passage. These were spatially corrected with hand-held GPS (Garmin etrex) at the cenotes (Fig. 2a).

2.2. Laboratory analyses

Each core was split, logged and analyzed for particle size at 1 cm resolution (with the exception of OC3). Particle sizes were measured using a Fraunhofer optical model of the Beckman Coulter LS230. Mean, median, mode and standard deviations were computed.

Petrographic analysis was also performed to document microfossil and calcite raft components with a sampling resolution of 5 cm. Approximately, 0.5 cm^3 of sediment was wet sieved using a 45 μm sieve to remove silts and clays and examined with a binocular dissecting microscope at 60–80X magnification. Foraminifera, testate amoebae and ostracods were counted and recorded as numbers of specimens per cm^3 (Scott and Hermelin, 1993). Since the determination of waterborne sedimentation was the focus of this study, the species were noted but not analyzed further. Calcite raft crystal habits (equant – prismatic vs acicular) were also documented along with the relative abundance of each form (no./cm^3). Cenote Borge, a site with a partially collapsed cavern ceiling, located approximately 30 Km SW of HN was used as a modern analog for the facies analysis (Fig. 3c–f).

Thirty-five AMS-radiocarbon dates were obtained on a variety of materials throughout the cores, targeting the interface between aquatic and subaerial sediments to obtain a basal age for flooding (Table 1). Seeds and fruit endocarps were preferentially selected where possible but twigs, charcoal and bulk organic matter (OM) were also used. Samples HN4 – HN12 were collected from ledges on the wall of HN at various water depths (Table 1).

Radiocarbon dates were calibrated using the northern hemisphere terrestrial calibration curve IntCal13.14C (Reimer et al., 2013) using the R-statistical software package Clam (Blaauw, 2010 v2.2; RStudio, 2014) and reported as ranges in calibrated years before present (cal BP) to the 2σ confidence interval.

3. Results

3.1. Cave facies

Four facies were recognized based primarily on sediment composition (OM and calcite rafts, mud) however; mean particle size, calcite raft abundance, crystal habits, and microfossils (ostracods, foraminifera and testate amoebae) also were utilized. Most cores showed a typical facies progression up-core (Figs. 4–7). These include: Mud, Seed, Calcite Raft, and an OM/Calcite Raft Facies. These are described in their stratigraphic order from bottom to top.

3.1.1. Mud facies (MF)

The carbonate MF, clay/silt sized limestone with a mean size of 4.7 μm, was found in four cores (C2, C4, C6 - Ich Balam, C7 - cave passage at edge of HN) (Fig. 4a, b). The MF generally lacked microfossils and had only small fragments of OM, although a few specimens of foraminifera were found in C2 and C4. Mud facies thickness was generally thin but variable in the cores, ranging from ≈ 5 cm in C6 to 23 cm in C7, which was entirely mud. The MF at the base of C4 may represent deposition in a pool of water on the cave bottom before full flooding of the cave, while the MF in C2 may represent mud deposition between limestone blocks of the breakdown pile in Ich Balam. C6 is more difficult to interpret as it is within the Calcite Raft (CR) facies, but again may be deposition between limestone boulders on the top of the breakdown pile. C7, taken near the edge of HN, consisted entirely of lime mud but contained small fragments of charcoal. This area was slightly depressed in the cave passage on the edge of HN and likely represents deposition when water level had risen to the base of the cave passage but not yet fully flooded it. The charcoal that was radiocarbon dated in C7 was likely reworked and out of context. However, in all these cases, the mud represents deposition in small isolated pools with limited inputs of sediment that probably originated from the overlying limestone during rainfall events.

3.1.2. Seed facies (SF)

The SF is characterized by seeds and fruit endocarps with undifferentiated OM and was found at the base of six cores (C1–5, 9; Fig. 4a, b). Two fruiting taxa dominate in this facies: *Byrsonima crassifolia* a member of the Malpighiaceae family, and *Thevetia peruviana* or yellow oleander, a species of Apocynaceae. Both are still common in the Yucatan (Morell-Hart, 2012). Ostracods were abundant in this assemblage, consisting of *Darwinula* spp. and *Cypridopsis* spp. Small numbers of foraminifera, including *Physalidia simplex* and *Conicosprillina* sp. were also present (n < 16; C1, C2 and C5; Fig. 5d–g). Acicular calcite rafts were present in most cores in addition to the equant - prismatic variety (Fig. 4a, b; Fig. 5a–c). The acicular rafts formed in the pore and interstitial space in the sediment or at the sediment/water interface and may be similar to the larger calcite florets from HN (Chatters et al., 2014). However, the presence of equant calcite rafts, which likely formed at the air/water interface, and the abundant ostracods indicate water was present, although shallow enough (likely <1 m) to allow piles of seeds and bat guano to form. These materials would become dispersed in deeper water (Fig. 3e). A modern analog was observed in Cenote Borge which shows a bat guano/seed pile (≈10–15 cm water depth) below an overhead rookery (Fig. 3c–e; Laprida, 2006; Taylor and Chafetz, 2004).

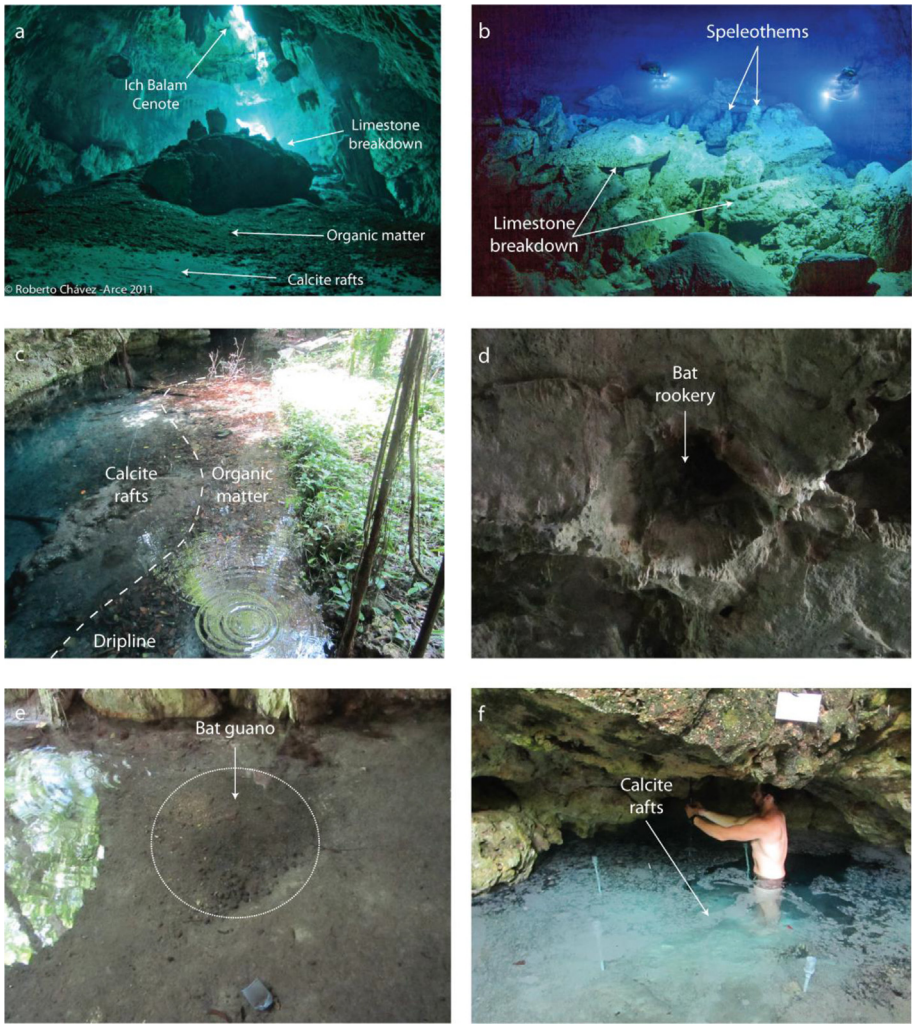

Fig. 3. a) View of Ich Balam looking up from the cave passage leading to HN. Note the size of the opening and the concentration of sediment on the central breakdown pile, as well as the calcite rafts forming on the surface water (white film) (Photo: Roberto Chávez-Arce). b) The bottom of HN showing the limestone boulders from ceiling collapse, the lack of sediment coverage and isolated speleothem. Divers are approx. 1.5 m in length. (Photo: Roberto Chávez-Arce). c) Cenote Borge showing the relationship between the cavern drip line and OM accumulations (note floating leaves. d) Bat rookery (overhead) e) guano pile including seeds and endocarps in Cenote Borge. Guano pile is approx. 40 cm wide and 15 cm high. f) Calcite raft formation in Cenote Borge - note white film on the surface.

3.1.3. *Calcite Raft Facies (CRF)*

The CRF consists of abundant calcite rafts that have well-developed equant – prismatic crystal habits with a mean particle size of 563 μm (Fig. 5a, b). This facies also contained variable abundances of ostracods, thecamoebians and foraminifera (Fig. 4a, b). The CRF had low OM content, consisting of ≈ 1–4 cm thick laminations/beds or occasional seed or wood fragments (e.g. C2, C5; Fig. 4a). CRF represents an increased water level from the SF but depth is difficult to estimate since calcite rafts formed at the surface can accumulate on the bottom over a range of water depths. Spatial and temporal calcite raft accumulation also requires suitable conditions to produce rafts. Changes in water chemistry, such as rates of CO_2 degassing, ionic concentration, temperature, pressure, fluid flow and magnesium concentration, have all been shown to have an influence on raft development but the process is still not well understood (González et al., 1992; Hanor, 1978; Jones et al., 1989; Palmer, 1996). However, on a physical basis, calcite raft formation requires the presence of air–water interface (e.g. air domes) so CO_2 degassing can occur and allow calcite to crystalize as rafts, in addition to water disturbances that cause these rafts to sink and accumulate on the bottom (e.g. water drips, water ripples etc.; Taylor and Chafetz, 2004). In Cenote Borge, rafts were only forming in one part of the water body when observed in May 2014 (Fig. 3f). The radiocarbon ages show variable accumulation rates from core to core suggesting that the focus of raft accumulation varied (e.g. C2 and C3). Particle sizes exhibit a general fining upwards in many of the Ich Balam cores (C1, C3, and C4) likely reflecting a change in water depth around the breakdown pile. As the water body increased in area from a ring surrounding the breakdown pile to a larger body of water when the central breakdown pile became flooded, it may have caused increased surface disturbance (i.e. ripples) preventing the rafts from attaining a larger size.

3.1.4. *Organic matter/Calcite rafts facies (OM/CRF)*

This mixed facies had high OM content, relative to the CRF, with a diverse assemblage of microfauna; ostracods (*Darwinula* spp. and *Cypridopsis* spp.), foraminifera (*Physalidia simplex* and *Conicosprillina* spp.) and thecamoebians (*Centropyxis aculeata*). The mean particle size (≈325 μm) was less than the CRF but greater than the SF (Fig. 4a, b).

The transition to the OM/CRF is due to the continued water level rise from CRF and is not present in all the cores (C2, C5, C7, C8 and

Table 1
Conventional and calibrated radiocarbon ages measured by atomic mass spectrometry from Cenote Ich Balam, Sac Actun Cave, Hoyo Negro and Cenote Oasis, Mexico.

Core/ Sample	Location	Sample depth (meters bmsl)	Depth in core (cm)	Material dated	Conventional radiocarbon age (14C yr BP)	δ13C (VPDB)	Laboratory code	Calibrated yrs BP (2σ confidence interval)
Core 1	Cenote Ich Balam	−11.5	64	Seed	7088 ± 31	−21.2	D-AMS 002363	7914–7970
Core 2	Cenote Ich Balam	−8.6	50	Seed	3565 ± 30	−34.2	D-AMS 002361	3822–3929
Core 2	Cenote Ich Balam	−8.9	79	Seed	5315 ± 30	−32.5	D-AMS 002365	5996–6186
Core 2	Cenote Ich Balam	−9.4	131	Seed	7270 ± 40	−26	Beta 333187	8009–8172
Core 3	Cenote Ich Balam	−10.9	8	Seed	5990 ± 32	−28.9	D-AMS 002371	6741–6911
Core 3	Cenote Ich Balam	−11.0	22	Seed	6400 ± 39	−33.5	D-AMS 002369	7268–7418
Core 3	Cenote Ich Balam	−11.2	38	Seed	6994 ± 31	−22.6	D-AMS 002368	7742–7817
Core 4	Cenote Ich Balam	−12.3	77	Seed	7269 ± 38	−21.9	D-AMS 002374	8010–8170
Core 5	Cenote Ich Balam	11.7	107	Seed	5909 ± 35	−26.9	D-AMS 002373	6658–6797
Core 5	Cenote Ich Balam	11.8	120	Seed	6300 ± 40	−24.4	Beta 333188	7163–7310
Core 6	Cenote Ich Balam	−4.9	26	Seed	3510 ± 31	−26.4	D-AMS 002372	3698–3865
Core 7	Cave Passage	−11.8	21	Charcoal	9941 ± 42	−21.8	D-AMS 003402	11242–11413
Core 9	Pit Core	−42.5	47	Seed1	8630 ± 50	−21.8	Beta 333189	9526–9700
Core 9	Pit Core	−42.5	47	Charcoal	9761 ± 33	−26.5	D-AMS 003403	11162–11240
Core 9	Pit Core	−42.5	47	Seed2	8826 ± 31	−33.8	D-AMS 003404	9731–9954
HN4	Pit Wall	−40.0	n/a	Wood	10467 ± 38	−32.1	D-AMS 003409	12372–12573
HN5	Pit Wall	−41.5	n/a	Wood	9761 ± 38	−29.7	D-AMS 003410	11145–11244
HN6	Pit Wall	−43.0	n/a	Wood	8935 ± 46	−29.4	D-AMS 003412	9912–10103
HN7	Pit Wall	−44.8	n/a	Wood	9793 ± 39	−29.4	D-AMS 003411	11176–11254
HN8	Pit Wall	−46.0	n/a	Wood	9626 ± 36	−31.7	D-AMS 003408	10786–10976
HN9	Pit Wall	−47.6	n/a	Wood	9557 ± 45	−26.9	D-AMS 003407	10918–11087
HN10	Pit Wall	−48.5	n/a	Wood	9416 ± 39	−31.7	D-AMS 003406	10562–10745
HN11	Pit Wall	−49.1	n/a	Seed	8667 ± 31	−32.3	D-AMS 003413	9546–9684
HN12	Pit Wall	−49.4	n/a	Seed	8815 ± 34	−26.6	D-AMS 003405	9696–9949
OAC2	Cenote Oasis	−4.1	66	Wood	4704 ± 29	−24.5	D-AMS 003397	5322–5418
OAC3	Cenote Oasis	−1.2	19	Seed	1090 ± 23	−31.5	D-AMS 003398	956–1058
OAC3	Cenote Oasis	−1.4	40	Seed	2049 ± 23	−27.4	D-AMS 003399	1946–2066
OAC3	Cenote Oasis	−1.6	62	Bulk OM	3129 ± 33	−27.2	D-AMS 003401	3317–3409
OAC3	Cenote Oasis	−1.8	76	Bulk OM	3887 ± 38	−15.7	D-AMS 003400	4230–4420
HN120512-2a[a]	HN floor guano pile 1	−48.0	n/a	Seed1	8925 ± 41	−26.5	D-AMS 02599a	9910–10200
HN120512-2b[a]	HN floor guano pile 1	−48.0	n/a	Seed2	8823 ± 48	n/a	D-AMS 02599b	9690–10155
HN120512-21[a]	HN floor guano pile 2	−48.0	n/a	Seed	8605 ± 45	−24.5	D-AMS 002600	9500–9685
HN130513-1[a]	HN floor guano pile 3	−48.3	n/a	Seed	8074 ± 37	−25.2	D-AMS 003374	8780–9125
HN130513-3[a]	HN floor guano pile 4	−37.1	n/a	Seed	8666 ± 38	−18.1	D-AMS 003375	9540–9700
HN130513-4[a]	HN floor atop HN56[b]	−46.1	n/a	Seed	9565 ± 37	−10.8	D-AMS 003373	10735–11095

[a] From Chatters et al. (2014); Table S3.
[b] Specimen from surface of bat guano partially covering a Tremarctos skull (skeletal group HN56).

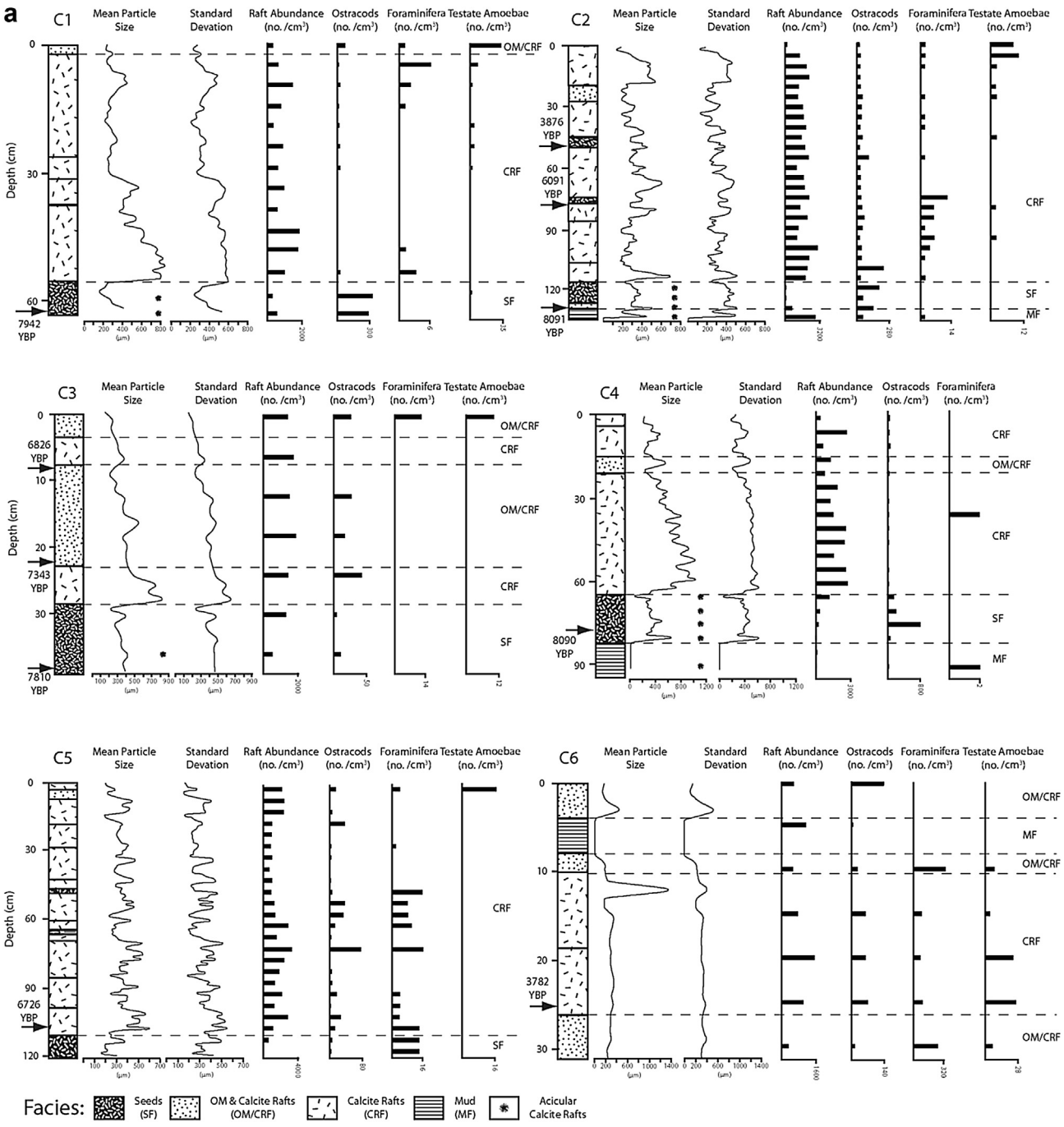

Fig. 4. a The core results including mean particle size (μm), standard deviation (μm), calcite raft abundance (no./cm^3), microfossils (no./cm^3), and radiocarbon ages for Cenote Ich Balam (C1-8), HN (C9) and Oasis (OC1-3). b The core results including mean particle size (μm), standard deviation (μm), calcite raft abundance (no./cm^3), microfossils (no./cm^3), and radiocarbon ages for Cenote Ich Balam (C1-8), HN (C9) and Oasis (OC1-3).

OC3). The OM/CRF is different from the SF as it contains more calcite rafts and a variety of OM (e.g. seeds, leaves, twigs, etc.). The higher OM content in this facies is likely from rising water levels creating a larger, deeper water body that redistributed the OM on the water surface and bottom. In Cenote Borge, coarse OM deposition (leaves and twigs) was focused in areas open to the surface with a transition to fine OM and calcite rafts coincident with the overlying drip line of the cavern (Fig. 3c). In Ich Balam, the small opening and cavern would focus OM sedimentation directly on the apex of the breakdown pile, with some downslope movement, but the low flow regime would allow only fine particulates to be transported deeper into the cave. In Oasis, the presence of a cave airway with lower water level would allow the OM to be distributed deeper into the cave but sedimentation would be increasingly restricted to the cenote as water level rose. The OM/CRF gets thicker towards the cenote opening and thinner with increasing distance from openings. The presence of airways would also allow deposition of bat transported OM, which would also be redistributed in a similar fashion (Fig. 4a, b).

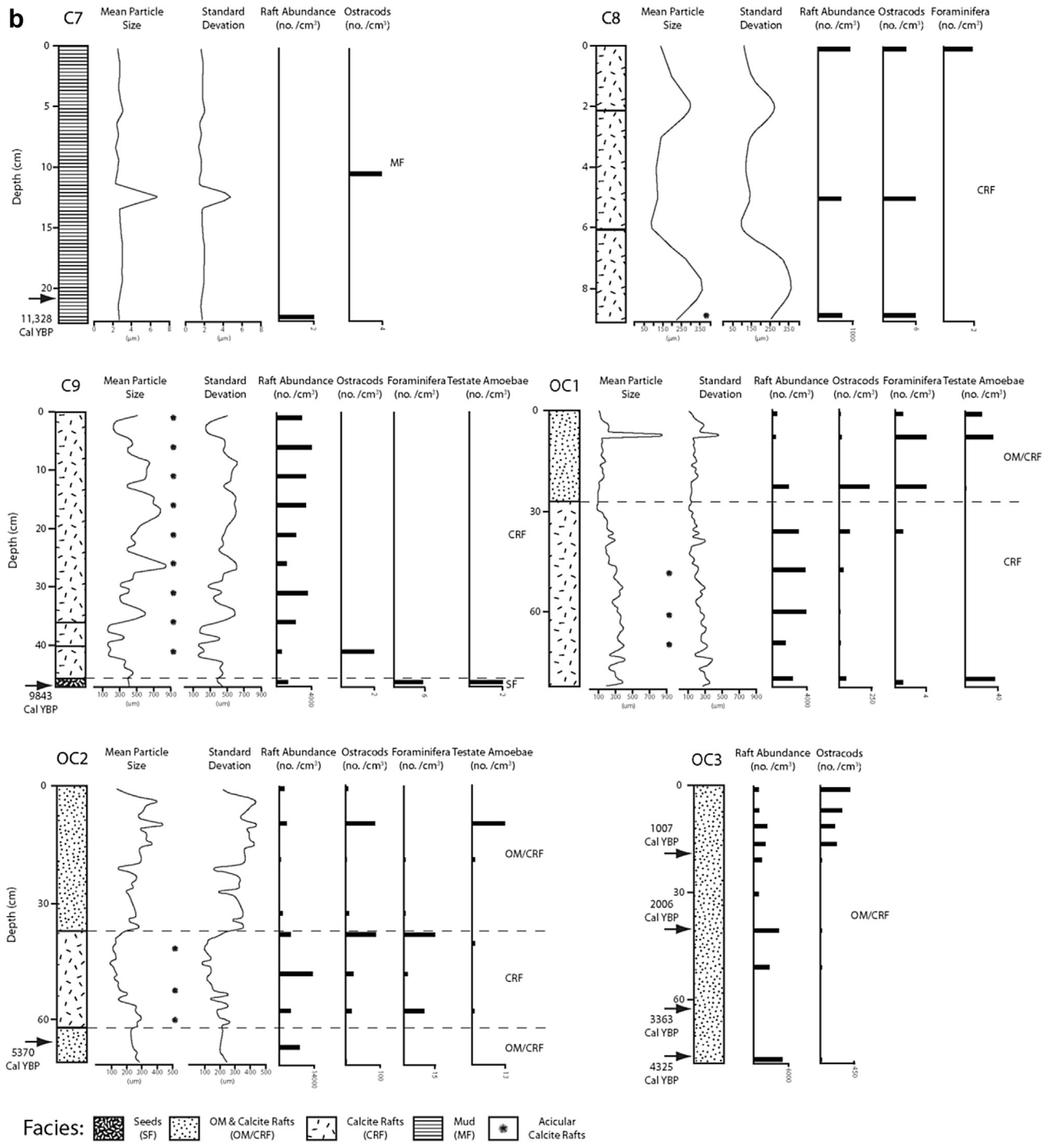

Fig. 4. (*continued*).

3.2. Radiocarbon ages

Twenty-nine radiocarbon dates obtained from sediment range from 1007 to 11,328 cal yr BP with no age reversals (Fig. 4a, b; Table 1). The ages from Ich Balam are older (3782–8090 cal yr BP) and deeper (mostly −9.6 to −12.3 m) compared to Oasis (1007–5370 cal yr BP; -1.8 to −4.1 m). The basal charcoal date of 11,328 cal yr BP from the lip of HN (C7) is the oldest radiocarbon date in the cores but is likely affected by reworking and/or an old wood effect. We have three ages for the HN core (C9), two on seeds (9526 – 9954 cal yr BP) and one older age on charcoal (11,162 – 11,240 cal yr BP) in addition to dates reported in Chatters et al. (2014) from guano piles (8953–10, 915 cal yr BP; Table 1). Again, the charcoal may reflect an old wood effect or be reworked or transported from an older deposit.

The surface samples collected from the ledges (n = 9) on the side of HN show age reversals with water depth. The radiocarbon samples were collected on lower ledges (≈ −40 to −49 m) of the bell-shaped pit (i.e. under an overhang), so seeds, twigs and charcoal could only lodge there if floating on the water surface. The OM

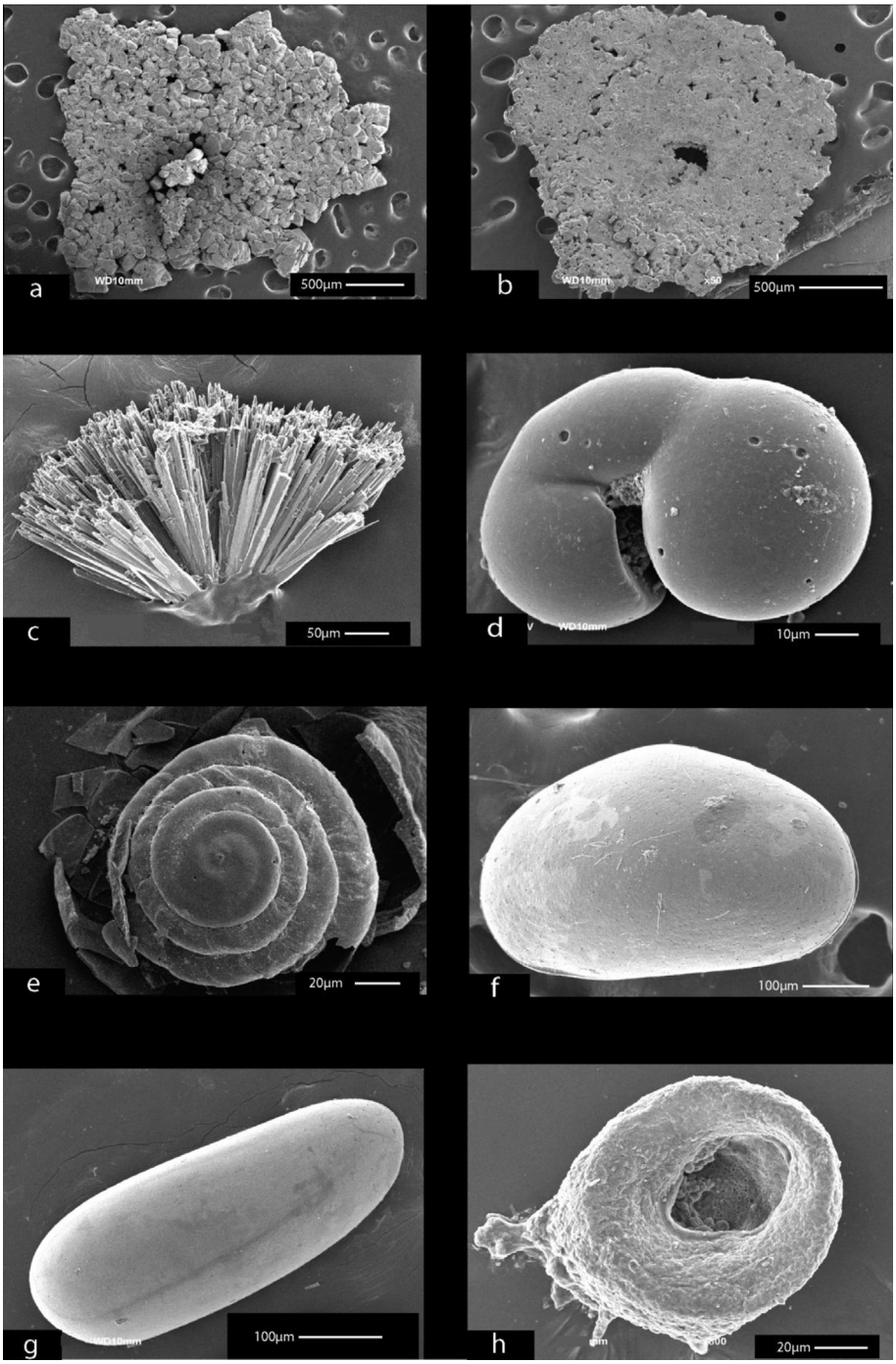

Fig. 5. a) Bottom surface of calcite raft showing irregular crystal terminations and equant calcite grains. b) Top surface of calcite raft showing fused fabric and smooth termination at air–water interface. c) Acicular calcite. d) *Physalidia simplex*. e) *Conicosprillina sp*. f) *Cypridopsis sp*. g) *Darwinula sp*. h) *Centropyxis aculeata*.

could only get to HN through large storm events, such as hurricanes, washing material originating from the cenotes into the pit. The age reversals indicate water level fluctuations in HN caused by these extreme rainfalls could have also refloated OM from the base or ledge (Collins et al., 2015a). The seeds and fruit endocarps ranged from 9600 to 9850 cal yr BP while the twigs and charcoal yielded older ages ranging from 10,000 to 12,500 cal yr BP. The seeds and endocarps likely were transported into HN by bats (guano piles dated from 8950 to 10,900 cal yr BP; Chatters et al., 2014, Table 1) while the twigs and charcoal may be allochthonous, having eroded from older deposits in the cenote and cave passages during large storm events.

3.3. Facies and water level reconstructions

Flooding history can be inferred from the elevations of basal radiocarbon dates for aquatic sediments with the underlying limestone providing the elevation. This dataset has one important caveat; aquatic sedimentation is not necessarily coincident with flooding since sediment deposition is controlled by the availability and transport of OM (bats or water) into the cave or the existence of

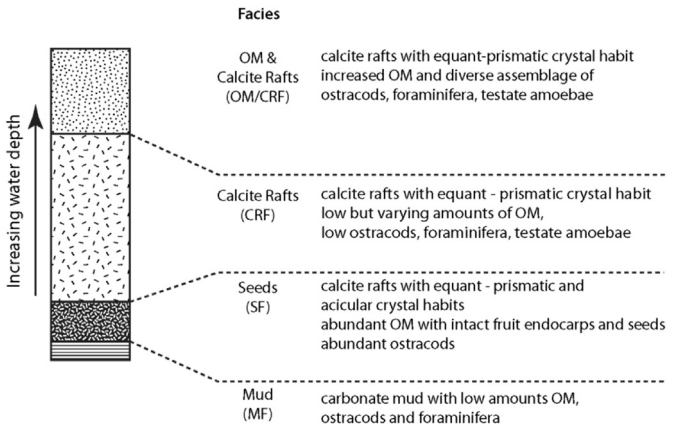

Fig. 6. Typical facies characteristics and stratigraphic position in this study.

suitable conditions for the formation and deposition of calcite rafts (e.g. water chemistry, air domes and water disturbance). Many caves in the Yucatan have been water filled for thousands of years but lack a sedimentary record of that inundation (Collins et al., 2015b). Therefore, basal radiocarbon ages on aquatic sediment may only provide a limit before which flooding occurred. This was addressed to some degree by taking numerous cores and using the oldest date for a given elevation to provide an age that approached the actual timing of flooding. The water level data were concentrated between −1.8 and −12.3 m in Cenotes Ich Balam and Oasis since they have the most sediment as a result of being open to the air and in proximity to OM inputs (Fig. 7b, c). The HN data were from a calcite raft core on the roof breakdown (C9; - 42.5 m) and from the ledge on the pit wall (≈−40 to −49 m). Many of the points coincide with documented Holocene sea-level rise, showing the influence of sea-level on water levels in the epikarst and cave (Fig. 7a, d). The Toscano and Macintyre model (2003) and the GIA (Glacial Isostatic Adjustment) model of Milne and Peros (2013) are similar over the past 9 Ka and were used to assess the relationship between cave flooding and sea-level (Fig. 7a–c). The ages (n = 8) of basal aquatic sediments in Ich Balam and Oasis generally follow sea-level rise although four dates are either too young (n = 2) or too old (n = 2) for their given elevation. As described, either sediment accumulation began after flooding (too young) or could have included reworked OM (too old) but four of the ages are coincident with the sea-level curves.

For HN we use Medina-Elizalde (2013) modeled relative sea-level curve (9–13 Ka), which has been GIA adjusted by 3.5 m (Chatters et al., 2014; Bard et al., 1990). The seed ages (SF; n = 2) from the base of aquatic sediment in C9 range between 9526 and 9954 cal yr BP matching the sea-level estimates. However, radiocarbon ages from the ledges vary, which, as discussed, is likely due to variation in water levels in the pit due to extreme precipitation events. For example, Hurricane Ingrid (Sept 2013) caused higher than normal water levels in the Tulum area cave systems (Collins et al., 2015a). In Yax Chen, instrumentally recorded water levels reached ~0.7 m above background levels, and a nearby cave system Temple of Doom had water levels that reached ~1.5 m above background and lasted for several days. This recent example demonstrates considerable regional variability, so it is uncertain how groundwater level in HN would have responded to storms when sea-levels were much lower. However, the upper cave passages entering HN may have acted as conduits, funneling water into the pit, raising water levels during rainfall events that may have lasted hours or days. The vadose porosity of the limestone would likely limit the flows; however, the flowstones developed on the floor of the cave passages would have occluded infiltration, enhancing flows in the cave passages leading to HN. The twigs, trunks and other OM found in HN which date from ~ 9 to 12 ka (Table 1) could have only arrived though wash-in events that occurred when the upper cave passage was dry, reinforcing this interpretation. High water levels in HN would not last long, but would allow OM to be deposited on higher than normal ledges on the pit wall.

Based on the water level reconstructions and the ceiling and bottom profiles of the cave, the pit was accessible until ≈8.1 Ka at which point water level in the passage reached the ceiling at HN proper restricting access to the pit. Continued water level rise eventually filled the cave passages as documented in the Oasis cores (OC1-3).

4. Discussion

The spatial and temporal distribution of sediment facies, along with the changing elevation of the base of aquatic sedimentation allowed the reconstruction of the water level history of HN and its connecting passages. Three intervals were recognized in this process.

4.1. Initial inundation of HN 9850–13,000 cal yr BP

In this early phase the upper cave passages, leading to HN were open to animals and humans, which could have entered from the three cenotes (Ich Balam, Oasis, La Concha; Figs. 8 and 9a). Ich Balam and Oasis are viewed as likely entry points since they have wide and easily navigated passages especially for the large gomphotheres. The basal core ages for Ich Balam indicate that the cenote opening was in existence at least by ≈ 8.1Ka, as entry of OM and bat guano could only occur if there was a karst window opening to the surface. However, it was likely open earlier (i.e. >13 Ka), as OM preservation is unlikely when the cenote was dry - i.e. decay would be rapid and OM accumulation would be thin and patchy (Collins et al., 2015a). Better OM preservation occurred with flooding of the upper passage, as will be discussed. One stick on the HN ledge dated to 12,372 - 12,573 cal yr BP. If it was transported into pit via the cave passage, Ich Balam represents the closest and most likely source of that material, thus extending the date to at least ≈13 Ka and the time Naia arrived in the pit.

Determining the water level history in HN is more difficult (Figs. 8 and 9a–d). Based on the correspondence of water level points from the shallower locations in Ich Balam and Oasis from which there were more data, it appears that flooding largely reflects rising Holocene sea-level (Fig. 7a). In HN however, the record appears to be more complicated due to the configuration of the cave passages and their relationship with the pit. Less data are available due to the lack of sedimentary deposits in HN, but also because earlier Holocene sea-level reconstructions have greater uncertainty due to the rarity of data and the high rate of sea-level rise during this period. Our basal age from the SF in C9 indicates that water was at −42 mbsl (and possibly higher) in HN at least by 9.5–10 Ka, but possibly earlier. Other bat guano deposits in HN date from 8.9 to 10.9 Ka (Table 1; Chatters et al., 2014), while the age range of the majority of OM on the ledges spans 9.5–11.2 Ka, which shows water, albeit with fluctuating levels, in HN as well.

The age of Naia (11.8–12.9 Ka; -42 mbsl) was determined through radiocarbon dating of her tooth, which was constrained with U–Th dates from calcite florets on her bones (≈9.5–12 Ka). Naia's skeletal condition indicated that she had fallen into water. Her disarticulated skeleton lacked evidence of serious impact trauma that would occur with a fall on a hard substrate (e.g. bone breaks or skull fractures). She and most other animal bones in the

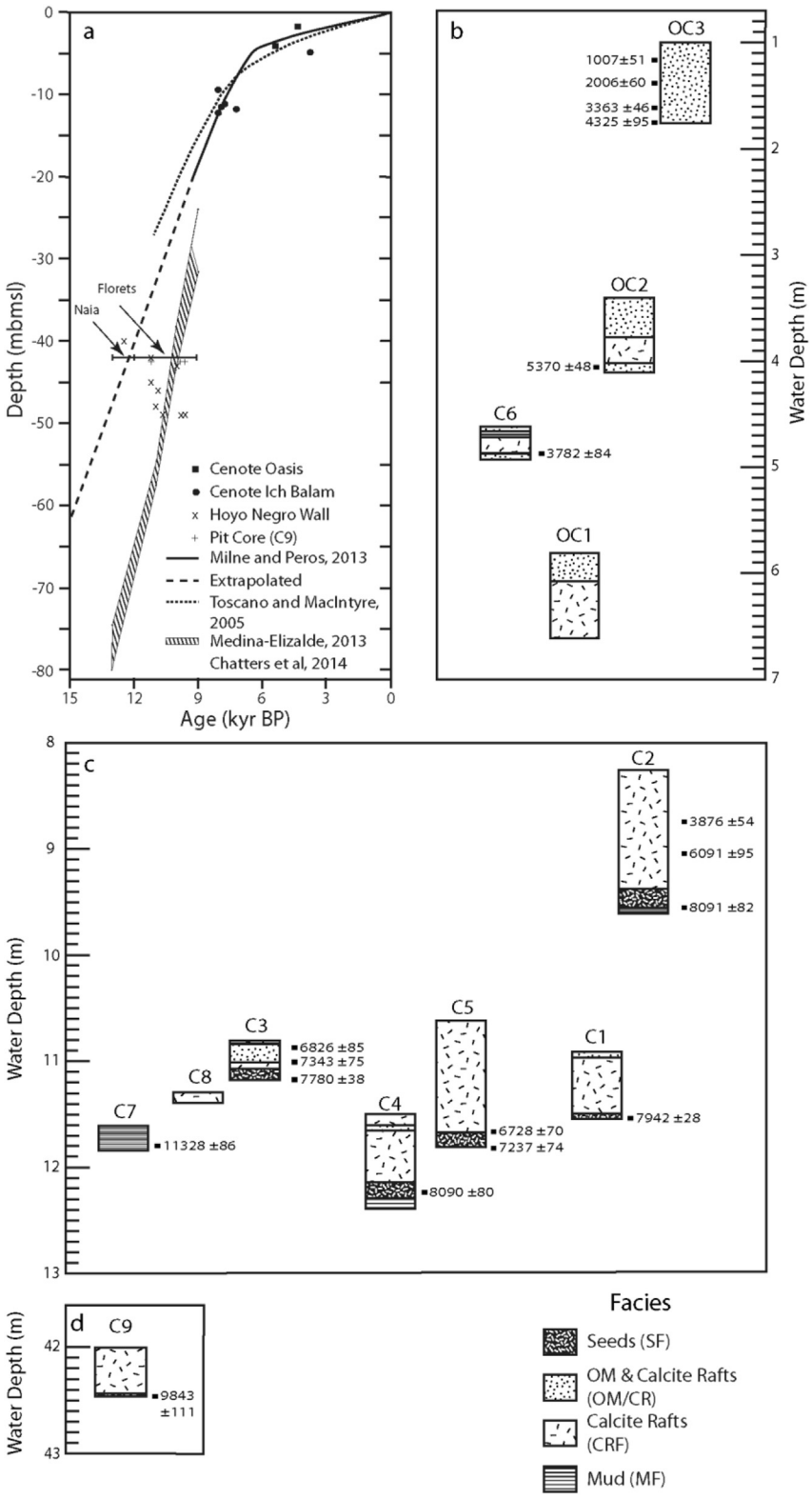

Fig. 7. Facies correlation from Cenotes Oasis (b) Ich Balam (c), and HN (d) showing rising water levels in the cave system and its relationship with Holocene sea-level rise (a). Basal radiocarbon ages on aquatic facies were used to reconstruct water levels.

pit also lack speleothem covering, supporting the theory that they fell into water or were quickly covered by rising water.

Our water level data fits well with the GIA corrected sea-level curve of Medina-Elizalde (2013) as presented in Chatters et al. (2014) but the skeletal taphonomy and age of Naia doesn't correspond as well. Sea-level and by correspondence water level in HN would have been −80 mbsl at 12–13 Ka, necessitating a short-term rise of 40 m in water level during rainfall events, which seems

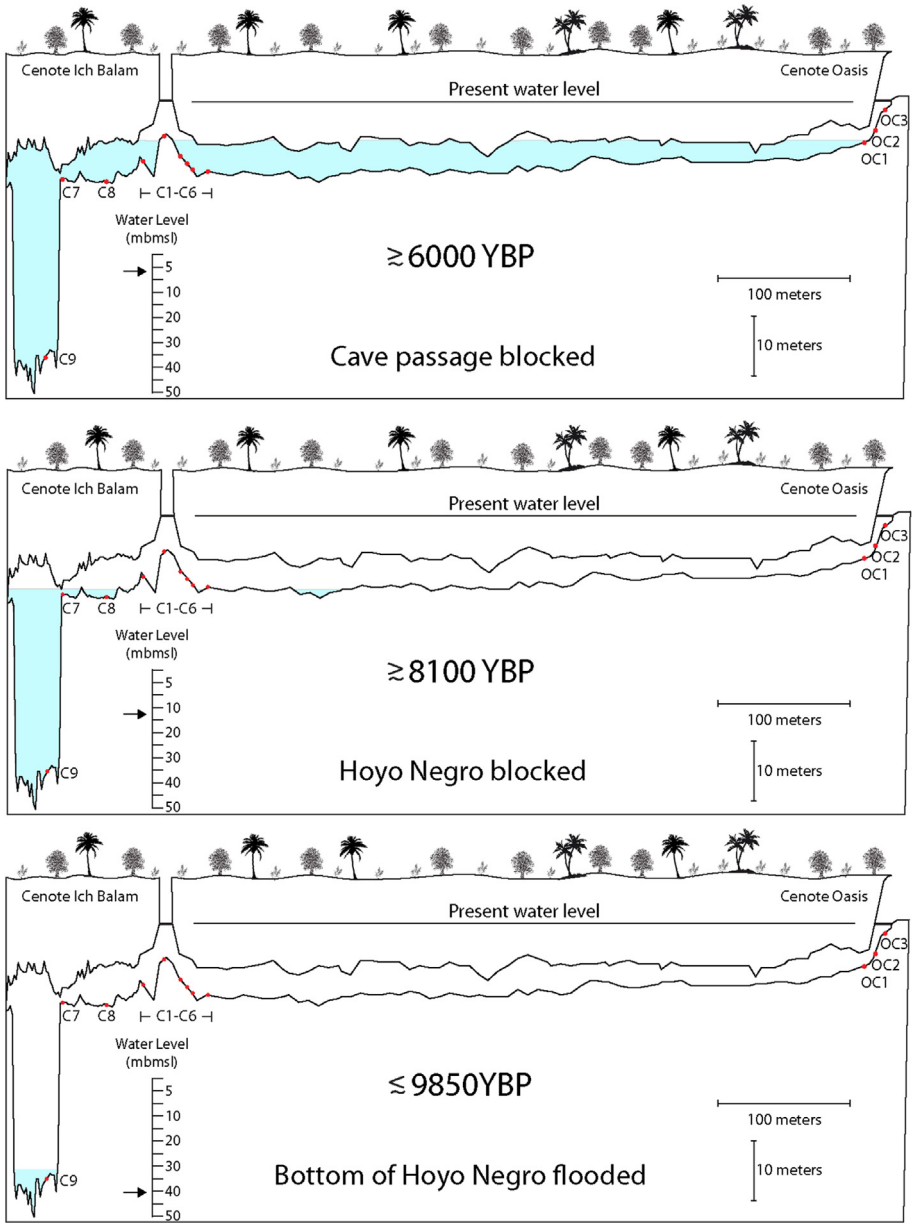

Fig. 8. Flooding history based on facies analysis and its relationship with measured cave ceiling and bottom elevations (vertical exaggeration = 10x).

unlikely due to the high permeability of Yucatan limestone. The Milne and Peros (2013), Caribbean derived GIA sea-level curve if extrapolated to 13 Ka fits the Naia data better as sea-level was close to 42 m at 13 Ka. However, the ledge data does not fit this curve well, since it means that the sampled OM is too young for a given depth and does not match the proposed model of deposition of floating OM on rising water levels during precipitation events (i.e. water levels will rise but not fall below base level). Medina-Elizalde (2013) fits the HN data better since there was OM on the ledges that are generally too old for a given depth. This argument assumes that OM deposition does not occur from above because of the overhang, although it is possible that turbulent currents in the pit could suspend and deposit OM on the ledges; however, floating OM is a more likely cause. There appears to be a disparity between the early flooding of the pit and later periods which better fit the Holocene sea-level curve. Gypsum and argillite beds from the Icaiche Formation may have acted as an aquitard allowing a localized perched water table in the pit during lower early Holocene sea-level (Perry et al., 2011). As sea-level rose and reached the more permeable upper limestone, the water table level more closely followed sea-level.

4.2. Rising water levels in HN 9850-8100 cal yr BP

Water levels continued to rise in HN, following Holocene sea-level change, with the CRF in C9 representing deepening water above −41 m after 9850 cal yr BP (Medina-Elizalde, 2013; Milne and Peros, 2013; Toscano and Macintyre, 2003). The majority of our radiocarbon ages from OM are older than 9.5 Ka but this is likely biased as we preferentially sampled guano piles that would have accumulated in shallow water and the OM from the ledges spanned only a short depth range over a short time period (40–49 m). As water levels in the pit increased, sediment would become more dispersed on the water surface and with sinking

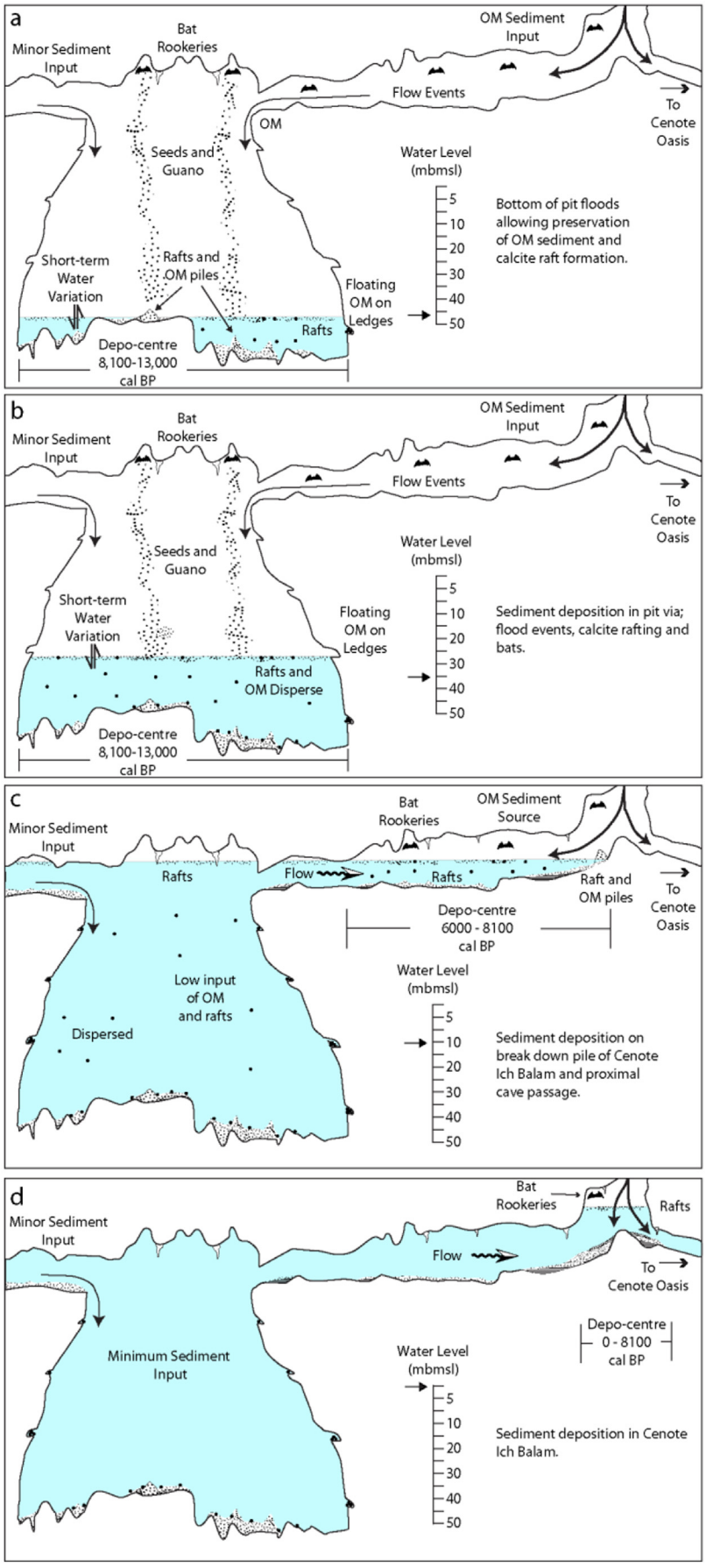

Fig. 9. a–d) Factors affecting sedimentation with rising water level in the cave.

would be more dispersed on the bottom of the pit (Gregory et al., 2015; Fig. 9b). The calcite raft piles could have accumulated over greater water depths because their formation would be based on suitable chemical conditions for their formation. However, the loci of deposition would be based on water disturbance (i.e. overhead drip water in HN), which would be static over periods of time. Further coring in the pit may provide more information on the spatial and temporal patterning of sedimentation in HN, but based on our data we assume that water levels steadily increased in the pit with episodic OM inputs from the cenotes and from overhead bat rookeries. Since HN would be isolated during rising water levels, all OM would be contained in the pit. The pit was the depo-center at this time but this changed when the floors of the cave passages leading to HN were flooded at ≈ 8.1 Ka (Fig. 9b, c).

4.3. Cave passages flooded >8100 cal yr BP

The upper cave passages leading to HN were flooded and continued to fill after 8.1 Ka, as documented in the Ich Balam stratigraphy (Figs. 8 and 9c). Soon after, access to HN would have been closed due to rising water levels reaching the cave ceiling at the pit. Evidence for the initial flooding comes from C7 on the rim of HN. This core was entirely muddy and represents ponding of water at the edge of HN as water levels rose prior to 8.1 Ka. Basal radiocarbon ages on bulk charcoal fragments provided an old age (11,162 - 11,240 cal yr BP) and there is extensive scatter of charcoal in this area. This charcoal could be from torches and fires used in the cave passage to access HN, but charcoal is easily floated and could be allochthonous (i.e. sourced from forest fires). The evidence of flooding is provided by the basal SF ages from Ich Balam. At this point the focus of deposition changed. HN was no longer accessible to humans or animals thus providing a minimum age for all of the mammalian skeletal material in HN (Figs. 8 and 9c). HN was also cut off from OM inputs brought in by bats or floated from cenotes during extreme events; however, the presence of an air dome in HN would still allow calcite raft deposition. Suspension transport of OM could still occur perhaps with extreme events but normal meteoric water flows are low with transport eastward from HN. Thus meteoric flow would transport sediment from Ich Balam and Oasis away from HN. This outcome is seen in our core data, which shows thicker OM sediment accumulation in cores downstream of Ich Balam. Input from upstream La Concha, which is >600 m away is not a likely contributor of OM sediment. Our radiocarbon ages of OM in the cave reflect that as well, with earlier ages in HN (≈9.5–11.5 Ka) relative to Ich Balam (≈3.8–8.1 Ka) As water levels in the cave passages reached ceiling heights, the depo-center would move closer to the open water areas in cenotes. Cave passages leading from Ich Balam and Oasis became further restricted by rising water levels and eventually became completely flooded by ≈ 6 Ka (Figs. 8 and 9d).

4.4. Comparisons with Green Bay and Walsingham Cave, Bermuda

Similar core studies conducted in Green Bay Cave in Bermuda show similar depositional patterns as Hoyo Negro (van Hengstum et al., 2011). Twelve cores were collected in a transect through the cave passage from Cliff Pool sinkhole to an opening in Harrington Sound. Most of the cores are at a similar depth of ~19–20 m below SL. The basal ages of calcite raft sediment shows an age that is too young by ~500–1000 yrs. for its elevation, indicating that there may have been water in the cave before calcite rafts began to form. Ceiling elevation fits better with the radiocarbon dated termination of calcite rafts deposition (Fig. 8; C5 in van Hengstum et al., 2011). Green Bay Cave also exhibits a shifting depo-center for OM sediment, which moved closer to the Cliff pool sinkhole as water level rose. Core one closest to the sinkhole has a radiocarbon age of ~3.1 Ka at 10 cm from the core top indicating that OM was being deposited further upslope and in the sinkhole itself with rising water level.

Walsingham Cave also shows departure between flooding ages from basal aquatic sediments and sea-level. A single core has a basal vadose facies that is overlain by an aquatic sediment facies (carbonate mud with foraminifera; Figs. 3 and 4 in van Hengstum et al., 2015b). The base of the carbonate mud has a radiocarbon age (~3 ka cal yrs BP) that is ~5 Ka too young for its elevation at ~ 20 mbsl (van Hengstum et al., 2015a, b).

5. Conclusion

This study inferred the water level history in HN and its connecting tunnels from the age and facies content of cave sediments. Water was continuously present in the bottom of HN at least by 9850 cal yr BP (C9) and maybe earlier based on the ledge data, which suggest that water was in the pit by 11 Ka. However, this age may be contaminated by the transport of old wood into the pit. The data matches Holocene sea-level rise of (Medina-Elizalde, 2013; GIA adjusted; Milne and Peros, 2013) indicating sea-level had a strong control on water level in the cave system, but the ledge data suggests short-term water level fluctuations from storms or hurricanes at least during the early Holocene. Blockage of the easiest access points (Ich Balam and Oasis) to HN occurred at ≈8.1 Ka as rising water levels reached the cave ceiling, providing a minimum age for the bone accumulation in the pit.

This study also emphasizes that sedimentation patterns in the cave environment are not controlled by water level alone (i.e. sea-level; van Hengstum et al., 2011). Cave passage morphology including floor and ceiling height, and water level, control sedimentation. As demonstrated here, the availability of airways strongly controlled OM sediment vectors; both surface floatation and bat transport. Likewise, the presence of airways and air domes affected calcite raft deposition. Cave sedimentation is therefore transient in space and time and multiple cores are required to determine a minimum age for chamber and passage flooding.

Acknowledgments

The authors would like to thank two anonymous reviewers for their comments and suggestions to improve the manuscript. Hoyo Negro is an official project of Mexico's National Institute of Anthropology and History (INAH), and the authors wish to thank the INAH Council of Archaeology. We gratefully acknowledge the support of: Global Underwater Explorers, The Mexican Cave Exploration Project (Fred Devos, Chris Le Maillot, S. Meecham, D. Riordan), Cindaq, and the staff at Zero Gravity for dive support and logistics. Ceiling and cave mapping was conducted by: Alex Alvarez, Roberto Chávez-Arce, Ali Perkins, Cameron Russo and the many volunteers on the Hoyo Negro Project. Special thanks to Onno van Eijk for coring assistance and Mallory Coles and Kate Slamon for sediment property analysis. Underwater photography courtesy of Roberto Chávez-Arce. DirectAMS provided radiocarbon dates on bat guano organics at no cost. Funding was provided by National Sciences and Engineering Research Council of Canada (EGR – Discovery: 5-35620); National Geographic Research and Exploration Grant (DR, JC, ANB, EGR); PADI Grant (SVC).

References

Anderson, D.G., Gillam, J.C., 2000. Paleoindian colonization of the Americas: implications from an examination of physiography, demography, and artifact distribution. Am. Antiq. 65 (1), 43–66.

Back, W., Hanshaw, B.B., Herman, J.S., Van Driel, J.N., 1986. Differential dissolition of a Pleistocene reef in the ground-water mixing zone of coastal Yucatan, Mexico. Geology 14, 137–140.
Back, W., Hanshaw, B.B., Pyle, T.E., Plummer, L.N., Weidie, A.E., 1979. Geo-chemical significance of groundwater discharge and carbonate dissolution to the formation of Caleta Xel Ha, Quintana Roo, Mexico. Water Resour. Res. 15, 1521–1535.
Bard, E., Hamelin, B., Fairbanks, R.G., Zindler, A., 1990. Calibration of the 14C timescale over the past 30,000 years using mass spectrometric U-Th ages from Barbados Corals. Nature 345, 405–410.
Bauer-Gottwein, P., Gondwe, B.R.N., Charvet, G., Marin, L.E., Rebolledo-Vieyra, M., Merediz-Alonso, G., 2011. Review: the Yucatan Peninsula karst aquifer, Mexico. Hydrogeol. J. 19, 507–524.
Beddows, P.A., 2004. Groundwater Hydrology of a Coastal Conduit Carbonate Aquifer: Caribbean Coast of the Yucatan Peninsula. Mexico Unpublished doctoral disertation. University of Bristol.
Blaauw, M., 2010. Methods and code for “classical” age-modelling of radiocarbon sequences. Quat. Geochronol. 5, 512–518.
Chatters, J.C., Kennett, D.J., Asmerom, Y., Kemp, B.M., Polyak, V., Blank, A.N., Beddows, P.A., Reinhardt, E., Arroyo-Cabrales, J., Bolnick, D.A., Malhi, T.R.S., Culleton, B.J., Luna Erreguerena, P., Rissolo, D., Morell-Hart, S., Stafford Jr., T.W., 2014. Late pleistocene human skeleton and mtDNA link paleoamericans and modern Native Americans. Science 344, 750–754.
Chatters, J.C., 2000. The recovery and first analysis of an early Holocene human skeleton from Kennewick, Washington. Am. Antiq. 65 (2), 291–316.
Coke, J., Perry, E.C., Long, A., 1991. Sea-level curve. Nature 353 (5), 25.
Collins, S.V., Reinhardt, E.G., Werner, C.L., Meacham, S., Devos, F., LeMaillot, C., 2015a. Hurricane ingrid sedimentation in Yax Chen cave system (Ox Bel Ha) Yucatan, Mexico. Palaeogeogr. Paleoclimatology Palaeoecol. (in press).
Collins, S.V., Reinhardt, E.G., Devos, F., LeMaillot, C., 2015b. Late holocene mangrove development and onset of sedimentation in Yax Chen cave system (Ox Bel Ha) Yucatan, Mexico. Palaeogeogr. Paleoclimatology, Palaeoecol. (in press).
Dixon, E.J., 1999. Bones Boats and Bison. Univesity of New Mexico Press, New Mexico.
Esterson, K., 2003. Mixing Corrosion in a Coastal Aquifer. Unpublished Masters of Science. Florida State University, p. 66.
Finch, W.A., 1965. The Karst Landscape of Yucatan. University of Illinois at Urbana-Champaign.
Gabriel, J.J., Reinhardt, E.G., Peros, M.C., Davidson, D.E., van Hengstum, P.J., Beddows, P.A., 2009. Palaeoenvironmental evolution of Cenote Actun Ha (Carwash) on the Yucatan Peninsula, Mexico and its response to Holocene sea-level rise. J. Paleolimnol. 42, 199–213.
González, A.H., Terrazas, A., Stinnesbeck, W., Benavente, M.E., Aviles, J., Rojas, C., Padilla, J.M., Velasquez, A., Acevez, E., Frey, E., 2013. The first humans in the Yucatan Penninsula found in drowned caves: the days of the late pleistocene-early holocene in a changing tropic. In: Graf, K.E., Ketron, C.V., Waters, M.R. (Eds.), Paleoamreican Odyssey. Center fo rthe Study of the First Americans, New Mexico, pp. 223–238.
González, A.H., Rojas Sandoval, C., Terrazas Mata, A., Benavente Sanvicente, M., Stinnesbeck, W., Aviles, J., Magdalena de los Rios, O., Acevez, E., 2008. The arrival of humans on the Yucatan Peninsula: evidence from submerged caves in the state of Quintana Roo, Mexico. Curr. Res. Pleistocene 25, 1–25.
González, L.A., Carpenter, S.J., Lohmann, K.C., 1992. Inorganic calcite morphology: roles of fluid chemistry and fluid flow. J. Sediment. Petrology 62, 382–399.
Gregory, B.R.B., Reinhardt, Eduard G., Gifford, J.A., 2015. The Influence of Morphology and Sea-rise on Sinkhole Sedimentation: Evidence from Little Salt Springs (submitted). McMaster University, Florida Masters, p. 26.
Hanor, J.S., 1978. Precipitation of beachrock cements: mixing of marine and meteoric waters vs. CO_2 -degassing. J. Sediment. Petrology 48, 489–501.
Hanshaw, B.B., Back, W., 1980. Chemical mass-wasting of the northern Yucatan Peninsula by groundwater dissolution. Geology 8, 222–224.
Hodell, D.A., Brenner, M., Curtis, J.H., 2005. Terminal Classic drought in the northern Maya lowlands inferred from multiple sediment cores in Lake Chichancanab (Mexico). Quat. Sci. Rev. 24, 1413–1427.
Jones, B., Renaut, R.W., Rosen, M.R., 1989. Trigonal dendritic calcite crystals forming from hot spring waters at Waikite, North Island, New Zealand. J. Sediment. Res. 70, 586–603.
Kambesis, P.N., Coke, J.G., 2013. Overview of the controls on Eogenetic cave and Karst development in Quintana Roo, Mexico. In: Lace, M.J., Mylroie, J.E. (Eds.), Coastal Karst Landforms, 5. Springer, Netherlands, pp. 347–373.
Laprida, C., 2006. Recent ostracods of the Pampas, Buenos Aires, Argentina: ecology and implications paleolimnological. Ameghiniana 43 (1), 1–27.
Medina-Elizalde, M., 2013. A global compilation of coral sea-level benchmarks: implications and new challenges. Earth Planet. Sci. Lett. 362, 310–318.
Milne, G.A., Peros, M., 2013. Data-model comparison of Holocene sea-level change in the circum-Caribbean region. Glob. Planet. Change 107, 119–131.
Moore, W.S., 1999. The subterranean estuary: a reaction zone of ground water and sea water. Mar. Chem. 65, 111–125.
Morell-Hart, S., 2012. Preliminary Analysis of Macrobotanical Samples from Hoyo Negro (TP-m 001.1). College of William and Mary, Quintana Roo.
Neuman, B.R., Rahbek, M.L., 2007. Modeling the Groundwater Catchment of the Sian Ka'an Reserve,. National Speleological Society, Quintana Roo.
Palmer, M.V., 1996. Influence of carbon dioxide outgassing rates ans accessory ions on calcium carbonate crystal shapes. In: Proceedings Geological Society of America, 28th Annual Meeting, 28, p. 48.
Peros, M.C., Reinhardt, E.G., Davis, A.M., 2007. A 6000-year record of ecological and hydrological changes from Laguna de la Leche, north coastal Cuba. Quat. Res. 67, 69–82.
Perry, E., Swift, J., Gamboa, J., Reeve, A., Sanborn, R., Marin, L., Villasuso, M., 1989. Geologic and environmental aspects of surface cementation, north coast, Yucatan, Mexico. Geology 17 (9), 818–821.
Perry, E., Marin, L., McClain, J., Velázquez, G., 1995. Ring of Cenotes (sinkholes), northwest Yucatan, Mexico: Its hydrogeologic characteristics and possible association with the Chicxulub impact crater. Geology 23 (1), 17–20.
Perry, E.C., Velazquez-Oliman, Socki, R.A., 2003. Hydrogeology of the Yucatan. In: 21st Symposium on Plant Biology. Arturo Gomez Pompa and Scott Fedick. The Haworth Press, Inc., 10 Alice Street, Binghamton, NY, pp. 115–138. Chapter 7.
Perry, E., Guadalupe, Velazquez Oliman, Wagner, N., 2011. Preliminary investigation of groundwater and surface water geochemistry in Campeche and Southern quintana roo. In: Spring, Ú.O. (Ed.), Water Resources in Mexico. Springer, Berlin, pp. 87–97.
Quintana Roo Speleological Survey, 2013. List of Long Underwater Caves in Quintana Roo, Mexico. Quintana Roo Speleological Survey, Tulum.
Reimer, P.J., Bard, M.G.L., Bayliss, A., Beck, J.W., Blackwell, P.G., Ramsey, C.B., Buck, C.E., Edwards, R.L., Freidrich, M., Groots, P.M., Guilderson, T.P., Haflidason, H., Hajdas, I., Hatté, C., Heaton, T.J., Hoffmann, D.L., Hogg, A.G., Hughen, K.A., Kaiser, K.F., Kromer, B., Manning, S.W., Nui, M., Reimer, R.W., Richards, D.A., Scott, E.M., Southon, J.R., Turney, C.S.M., van der Plicht, J., 2013. IntCal13 and Marine13 radiocarbon age calibration curves, 0-50,000 years Cal BP. Radiocarbon 55, 1896–1887.
RStudio, 2014. RStudio: Integrated Development Environment for R (Version 0.98.1062) [Computer software]. Boston, MA. Retrieved Jan 5, 2014. Available from: http://www.rstudio.org/.
Scott, D.B., Hermelin, J.O.R., 1993. A device for precision splitting of micropaleontological samples in liquid suspension. J. Paleontology 67, 151–154.
Smart, P.L., Beddows, P.A., Coke, J., Doerr, S., Smith, S., Whitaker, F.F., 2006. Cave development on the Caribbean coast of the Yucatan Peninsula, Quintana Roo, Mexico. In: Harmon, R. S. a. C. W., (Ed.), Perspectives on Karst Geomorphology, Hydrology and Geochemistry - a Tribute Volume to Derek C. Ford and William B. White, 404, pp. 105–128. Geological Society of America Special Paper.
Taylor, P.M., Chafetz, H.S., 2004. Floating rafts of calcite Crystals in cave pools, Central Texas, USA: Crystal habit vs. Saturation state. J. Sediment. Res. 74 (3), 328–341.
Taylor, R.E., 2009. Six Decades of radiocarbon dating in new world Archaeology. Radiocarbon 51 (1), 173–212.
Toscano, M.A., Macintyre, I.G., 2003. Corrected western Atlantic sea-level curve for the last 11,000 years based on calibrated 14C dates from Acropora framework and intertidal mangrove peat. Coral Reefs 22, 257–270.
van Hengstum, P.J., Donnelly, J.P., Kingston, A.W., Williams, B.E., Scott, D.B., Reinhardt, E.G., Little, S.N., Patterson, W.P., 2015a. Low Frequency Storminess at Bermuda Linked to Cooling Events in the North Atlantic Region (in press).
van Hengstum, P.J., Donnelly, J.P., Toomey, M.R., Albury, N.A., Lane, P., Kakuk, B., 2013. Heightened hurricane activity on the Little Bahama Bank from 1350 to 1650 AD. Cont. Shelf Res. 86, 103–115.
van Hengstum, P.J., Richards, D.A., Onac, B.P., Dorale, J.A., 2015b. Coastal caves and sinkholes. In: Shennan, Ian, Long, A.J., Horton, B.J. (Eds.), Handbook of Sea-level Research. John Wiley and Sons Ltd.
van Hengstum, P.J., Scott, D.B., Grocke, D.R., Charette, M.A., 2011. Sea level controls sedimentation and environments in coastal caves and sinkholes. Mar. Geol. 286, 35–50.
van Hengstum, P.J., Scott, D.B., Javaux, E.J., 2009a. Foraminifera in elevated Bermudian caves provide further evidence for +21 m eustatic sea-level during Marine Isotope Stage 11. Quat. Sci. Rev. 28, 1850–1860.
van Hengstum, P.J., Reinhardt, E.G., Beddows, P.A., Schwarcz, H.P., Gabriel, J.J., 2009b. Foraminifera and testate amoebae (thecamoebians) in an anchialine cave: surface distributions from Actun Ha (Carwash) cave system, Mexico. Limnol. Oceanogr. 54 (1), 391–396.
van Hengstum, P.J., Reinhardt, E.G., Beddows, P.A., Huang, R.J., Gabriel, J.J., 2008. Thecamoebians (testate amoebae) and foraminifera from three anchialine cenotes in Mexico: low salinity (1.5-4.5 psu) faunal transitions. J. Foraminifer. Res. 38 (4), 305–317.
van Hengstum, P.J., Reinhardt, E.G., Beddows, P.A., Gabriel, J.J., 2010. Linkages between Holocene paleoclimate and paleohydrogeology preserved in a Yucatan underwater cave. Quat. Sci. Rev. 29 (19–20), 2788–2798.
Ward, W.C., Keller, G., Stinnesbeck, W., Adatte, T., 1995. Yucatan subsurfacce stratigraphy: implications and constraints for the Chicxulub impact. Geology 23 (10), 873–876.
Weidie, A.E., 1985. Geology of Yucatan Platform: Part 1, p. 19.
Werner, C., 2007. Double-diffusive Fingering in Porous Media. Unpublished doctoral dissertation. Florida State University, United States, p. 114.